

High-resolution topography of Gusev crater using CTX data (Mars)

Topografía de alta resolución de cráter Gusev a partir de datos CTX (Marte)

Ronny Steven Anangonó-Tutasig^{1*}, Francisco Javier De Cos Juez¹, Susana Fernández Menéndez¹

¹Instituto Universitario de Ciencias y Tecnologías Espaciales de Asturias (ICTEA), C. Independencia 13, E-33004 Oviedo.

anangonoronny@gmail.com *, fjc@uniovi.es, fernandezmsusana@uniovi.es

*Corresponding author

ABSTRACT

High-resolution Digital Terrain Models (DTMs) of Mars are both limited and crucial for studying surface processes. The available DTMs generated from Mars Orbiter Laser Altimeter (MOLA) and High-Resolution Stereo Camera (HRSC) data offer limited resolution for working on a metre scale. The MER-A mission's exploration of the Gusev crater was based on the data provided by MOLA and HRSC. However, with the introduction of the stereoscopic images obtained by the Context Camera (CTX) on board the Mars Reconnaissance Orbiter (MRO), it has been possible to generate topographic data with greater detail, significantly improving the MOLA and HRSC data. This has resulted in the generation of new DTMs with a resolution of ~5 m/pixel. Comparative analysis of these CTX DTMs with the MOLA and HRSC data provides an updated perspective of the Gusev topography and its geological features. The prominent advantage of using CTX stereo images lies in their wide coverage, as they have mapped 99.9% of the Martian surface. This wide coverage allows the creation of high-resolution models that will prove invaluable for future studies and missions.

Key-words: Crater, Mars, Topography, Morphology, Digital Terrain Model (DTM).

RESUMEN

Los Modelos Digitales del Terreno (MDT) de alta resolución de Marte son tan escasos como cruciales para estudiar los procesos de la superficie. Los MDT disponibles generados gracias a los datos obtenidos por el Mars Orbiter Laser Altimeter (MOLA) y la High-Resolution Stereo Camera (HRSC) ofrecen una resolución limitada para trabajar a escala métrica. La exploración del cráter Gusev, realizada por la misión MER-A, se basó en los datos proporcionados por MOLA y HRSC. Sin embargo, con la introducción de las imágenes estereoscópicas obtenidas por la Cámara de Contexto (CTX) a bordo de la Mars Reconnaissance Orbiter (MRO), se ha podido generar datos topográficos con mayor detalle, mejorado significativamente a los datos MOLA y HRSC. Esto ha dado lugar a la creación de nuevos MDT con una resolución de ~5 m/píxel. El análisis comparativo de estos MDT CTX con los datos de MOLA y HRSC proporciona una visión actualizada de la topografía de Gusev y de sus características geológicas. La principal ventaja de utilizar imágenes estereoscópicas CTX reside en su amplia cobertura, ya que han cartografiado el 99,9% de la superficie marciana. Esta amplia cobertura permite crear modelos de alta resolución que resultarán muy valiosos para futuros estudios y misiones.

Palabras clave: Cráter, Marte, Topografía, Morfología, Modelo Digital del Terreno (MDT).

Geogaceta, 75 (2024), 91-94

<https://doi.org/10.55407/geogaceta100671>

ISSN (versión impresa): 0213-683X

ISSN (Internet): 2173-6545

Fecha de recepción: 30/06/2023

Fecha de revisión: 24/10/2023

Fecha de aceptación: 24/11/2023

Introduction

Mars has been 99.9% mapped by the context camera (CTX) (Malin *et al.*, 2007) on board the Mars Reconnaissance Orbiter (MRO), which provides images with a resolution of ~5 m/pixel, essential for mapping work. However, Mars currently lacks the highest-resolution digital terrain models (DTMs) due to the high computing resources required for their processing. DTMs generated at such resolutions have primarily focused on regions of interest for future missions. Many of these available DTMs have been produced by multiple research groups. Utilizing data collected by the Mars Orbiter Laser Altimeter (MOLA) instrument on board the Mars Global Surveyor (MGS), a global terrain

model of Mars was created with a resolution of 200-400 m/pixel (Smith *et al.*, 2001; Laura and Ferguson, 2016). Data obtained from the High-Resolution Stereo Camera (HRSC) instrument on the ESA's Mars Express mission also created to terrain models with a resolution of ~75 m/pixel (Gwinner *et al.*, 2016). Nevertheless, both terrain models have limited resolution for metric-scale investigations of the Martian surface within the Gusev crater region (Fig.1).

Gusev Crater, located at 14.64°S and 175.36°E in the southern hemisphere of Mars, has a diameter of ~166 km. This crater was the landing site of the MER-A NASA mission in 2004. The rover Spirit's investigations primarily focused on seeking clear evidence of past water presence on Mars.

Methodology

To generate this new topography, we used the open-source software available from NASA, Integrated software for Imagers and spectrometers (ISIS), version 7.0.1 (Anderson *et al.*, 2004; Anderson, 2008), and Ames Stereo Pipeline (ASP), version 3.2.0 (Moratto *et al.*, 2010; Beyer *et al.*, 2018).

In this study, the processing of these new DTMs has been automated using ISIS and ASP commands (Fig.2). The pre-processing of these images is carried out with the ISIS tools, to convert the images into the input format for stereo (IMG. to .cub). The mroctx2isis tool converts the images into .cub files. Spicinit provides spacecraft camera positions, body shape, and orientation to calculate ground positions

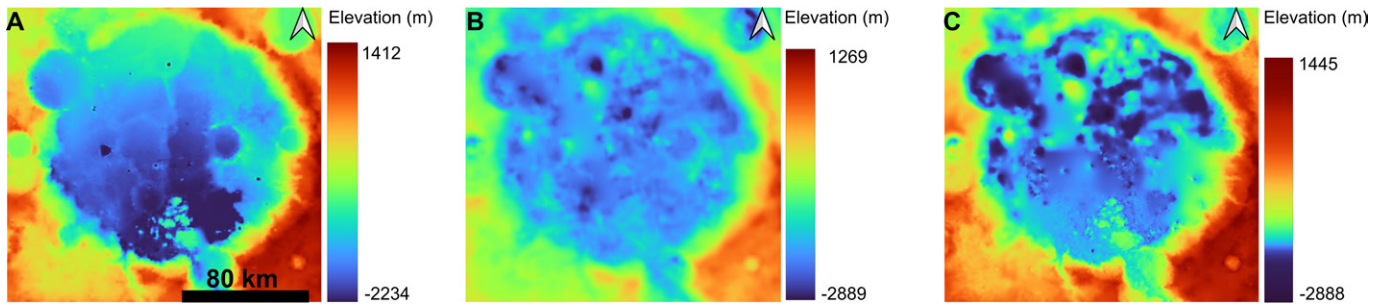


Fig. 1.- Digital elevation models available for Gusev crater. A) DTM MOLA (400 m/pixel). B) DTM HRSC (400 m/pixel). C) DTM MOLA-HRSC (200 m/pixel). Gusev crater diameter: ~166 km. See color figure in the web.

Fig. 1.- Modelos digitales de elevación disponibles para cráter Gusev. A) DTM MOLA (400 m/píxel) B) DTM HRSC (400 m/píxel) C) DTM MOLA-HRSC (200 m/píxel). Diámetro del cráter Gusev: ~160 km. Ver figura en color en la web.

(LAT/LON) and photometric angles. Ctxcal performs radiometric corrections for both stereo images. Ctxevenodd removes the effects that occur in the par/im-pair bands of the context camera.

The ASP tool cam2map4stereo calculates the minimum overlap between the two images to project the two images. The default is a sinusoidal projection (Beyer *et al.*, 2018). Depending on the location of the images on Mars (poles, hemisphere, equator), a more suitable projection can be assigned.

ASP's bundle_adjust tool, which is based on non-linear least squares algorithms (Ceres Solver algorithm), iterates through a least-cost function to minimize the triangulation error between the camera positions and the thousands of pixels in the scene previously generated (Beyer *et al.*, 2018), reducing the error between the back-projected pixel location and its actual location on the surface (Triggs *et al.*, 2000), avoiding distortion of the images as much as possible.

The parallel_stereo tool processes the stereo images that have been previously corrected, producing an output point cloud for each image, which can then be further processed into a mesh for display. The steps executed by parallel_stereo is described below:

Preprocessing: normalize the two input images, identify the points of interest (pixels), match both images while calculating the convergence angle for this stereo pair.

Stereo correlation: Generates an image where pixels describe their position in all three axes (LAT/LON/ELEV) and the horizontal and vertical displacement between the stereo images. The stereo algorithm distributes the process between this and subsequent stages (Beyer *et al.*, 2018).

Blending: Uses a sub-pixel refinement algorithm to adjust the valid pixels generated in the previous stage. This generated pixel uses as reference the eight neighboring pixels to perform the correlation between the pair images (Beyer *et al.*, 2018).

Sub-pixel refinement: Performs a filtering of outliers and matching errors generated by the previous step. Pixels may be invalid due to large differences between the two stereo images (e.g., quality and resolution of the images, smooth surfaces with a low signal-to-noise ratio).

Outlier removal: Performs outlier filtering and, in turn, fills holes using in-painting algorithm (Xia, *et al.*, 2008), which identifies areas in the image that require filling or restoration. These areas

are filled from neighboring pixel information, which extracts features such as textures, colors, and gradients, which will be used to guide the filling process.

Triangulation: Generates a 3D point cloud from a previously filtered and corrected scene by intersecting rays traced from the cameras, describing the 3D location of each matched pixel for each image (Beyer *et al.*, 2018). Using the nearest neighbor algorithm, the pc_align tool aligns the point cloud with a reference DTM (e.g., MOLA, HRSC) by means of least squares. The point2dem tool takes the point cloud and generates a DTM in GeoTIFF format, which can then be exported for viewing and working within a GIS environment.

The result is a DTM with a resolution of ~5 m/pixel. With modifications to the code parameters, the final product can be refined. Each parameter can be found in more detail in the ASP guide that has been used in this section (Beyer *et al.*, 2018).

Results

With these new CTX's DTMs we have compared a series of morphologies. In all cases, we have obtained more detailed information about the topography of this crater.

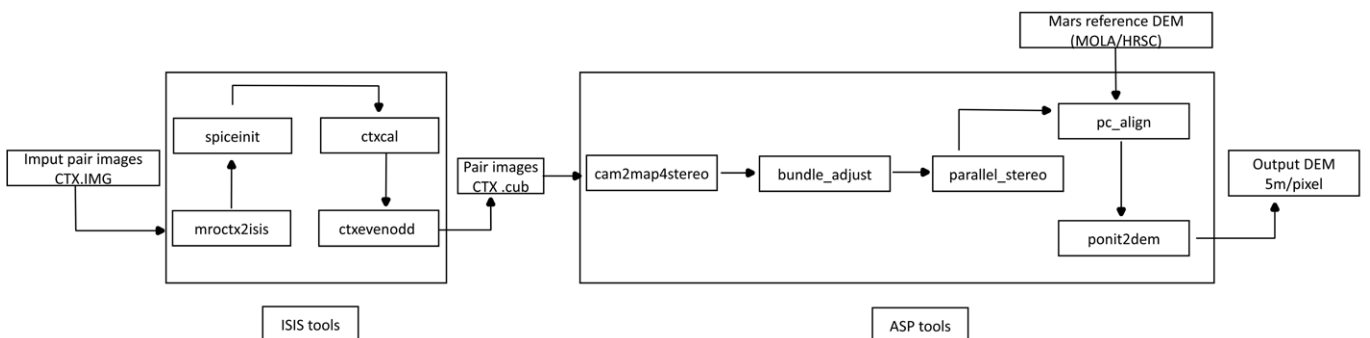


Fig. 2.- The workflow for processing CTX stereo image pairs and DTM output.

Fig. 2.- El flujo de trabajo para el procesamiento de los pares de imágenes estéreo CTX y salida del MDT.

On the surface of Gusev Crater, there are ridges extending across the surface, generally oriented in a north-south direction. Grin and Cabrol, (1997) suggested that these ridges result from rotational currents beneath a paleolake within Gusev in glacial periods. However, they do not provide evidence of "rotational" orientation changes around Gusev (Milam *et al.*, 2003). Some points along these ridges rise as much as 200 m above the surface of Gusev and extend for several kilometers. In the CTX DTM, maximum elevations of -1850 m have been extracted, whereas the MOLA DTM records elevations of -1837 m (Fig. 3.A). This new CTX DTM preserves the morphological characteristics of the CTX image, obtaining more information on/about these features in comparison with the MOLA and HRSC data. With these updated topographic data, we can gain a more detailed understanding of the morphology of these ridges.

Other morphological features observed on the surface of Gusev crater include small impact craters (<10 km diameter), in contrast to larger craters like Thira (~20 km diameter) or Gusev (~166 km diameter). In CTX images, we can discern their morphological characteristics such as shape and size, but we lack more detailed topographic data, such as crater depth and the slope of inner walls. The available MOLA and HRSC data do not provide insights into the topographic characteristics of these features. To the W of the MER-A landing ellipse is the Crivitz crater, a complex crater due to its morphological characteristics (French, 1999), making unique within in Gusev crater (see fig. 3.B). Although Crivitz crater has been mapped in studies by Kuzmin *et al.*, (2000) and Milam *et al.*, (2003), it lacks a detailed description. This crater has a diameter of ~6 km, with a circular morphology and characteristic central peak. Our CTX DTM obtains great results when compared to the topography recorded by MOLA and HRSC (fig. 3.B). In the CTX DTM a topographic profile has been plotted, where we have extracted the height of the central peak, with values of -2307 m. In the DTM MOLA and HRSC we do not have this information, so the CTX DTM provides us with much more information, an invaluable source of additional information that even reshapes our understanding of the morphology of this specific crater.

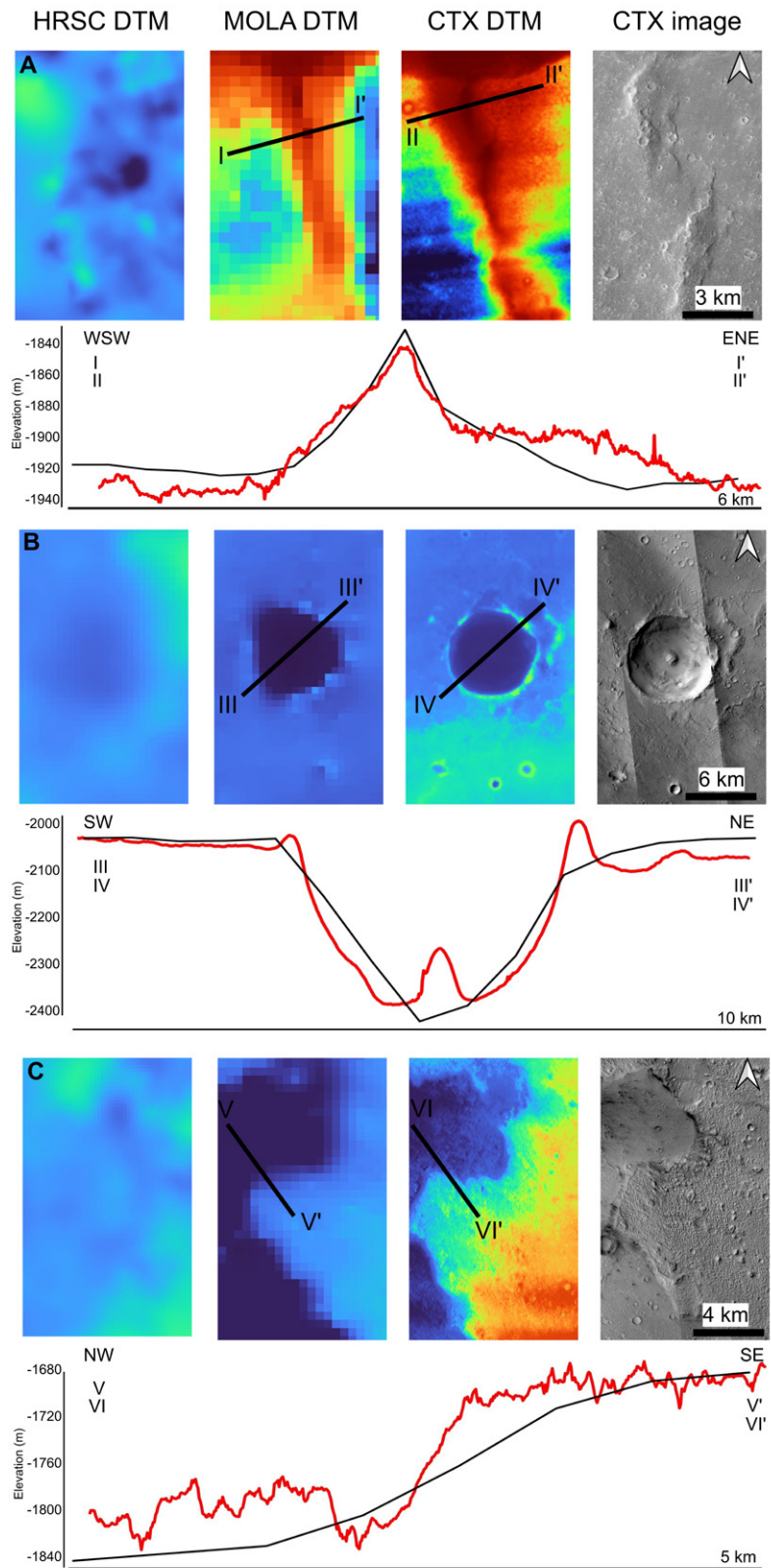


Fig. 3.- Reconstruction of the high-resolution topography of the Gusev crater using CTX images and comparison with available data. The topographic profiles correspond to MOLA topography (black colour) and CTX DTM (red colour): A) Gusev crater ridges. B) Crivitz crater. C) Channeled shapes. As we can see, in all the images we obtain better results in the CTX DTM with respect to the HRSC and MOLA DTM. See color figure in the web.

Fig. 3.- Reconstrucción de la topografía en alta resolución de cráter Gusev mediante imágenes CTX y su comparación con los datos disponibles. Los perfiles topográficos corresponden a la topografía MOLA (color negro) y MDT CTX (color rojo): A) Crestas de cráter Gusev. B) Cráter Crivitz. C) Formas canalizadas. Como podemos ver, en todos los casos obtenemos mejores resultados (resolución en elevación) en el MDT CTX con respecto a los MDTs derivados de los datos de HRSC y MOLA. Ver figura en color en la web.

To the SE of the main crater, near the delta, channel-like morphologies are visible (see Fig. 3.C), likely shaped by the action of some fluid in the past. Kuzmin *et al.*, (2000) suggest that these morphologies correspond to fluvio-lacustrine deposits. Milam *et al.*, (2003) identify these channel-like features as the contact between morphological units (ETm-WRm units as described in their study). These channel-like morphologies measure between 100 m and 500 m in width. The lowest elevation of these channels is -1790 m, with a depth of ~40 m relative to the outer edges at -1750 m (see Fig. 3.C). As a result, we observe that these DTMs provide higher resolution and better delineation of the morphology of these features compared to MOLA and HRSC data. With this new topographic data regarding the depth of these channel-like features, we can know deeper into the study of how these channels were formed, where water likely played a significant role.

Conclusions

Our new CTX DTMs, with a resolution of ~5 m/pixel, provide detailed topographic information for Gusev crater. This information is unavailable in the MOLA and HRSC datasets due to their limited spatial resolutions (200 m/pixel and 400 m/pixel, respectively). These high-resolution datasets allow for a more comprehensive exploration of the surface's topographic details, especially those at a metric scale, including channel-like formations, crater floors, and features such as ridges, as discussed in the results section. One of the primary advantages of these CTX DTMs is their faithful preservation of the morphological characteristics observed in CTX images, in addition to obtaining new topographical data. When comparing the elevations calculated in the three geological features compared between the MOLA and CTX DTM data, we see that there is no great disparity between the topographic data (~15 m), as the MOLA data has a vertical accuracy of ± 1.5 m. We consider that this new DTMs can help to perform more new detailed surface studies in the Gusev area. They offer a fresh perspective on the surface processes taking place within the crater, as well as the geological features that exist.

Data availability

The CTX stereo images are available in the database [Planetary Image Locator Tool](#) of the Planetary Data System (PDS) node. The [Integrated Software for Imagers and Spectrometers](#) (ISIS) and [Neo-GeographyToolkit/StereoPipeline](#) (ASP) software can be found in the GitHub repository. The code used as well as the generated data can be obtained from the author of this article.

Authors' contribution

Ronny Steveen Anagonó-Tutasig: Testing and execution of the code, writing. **Susana Fernández Menéndez:** Thesis supervisor, writing, structure review and corrections. **Francisco Javier de Cos Juez:** Thesis supervisor, research fundraiser.

Acknowledgements

This work was supported by funding AYUD/2021/51301, support for research groups from organizations in the Principality of Asturias for the period 2021-2023. To Dr. Erica Luzzi for her help with the familiarization of the code. We appreciate the reviewers of this article for their work.

References

- Anderson, J. *et al.* (2004) 'Modernization of the Integrated Software for Imagers and Spectrometers', *Lunar Planet. Sci.*, 35.
- Anderson, J.A. (2008) 'ISIS Camera Model Design', p. 2159.
- Beyer, R.A., Alexandrov, O. and McMichael, S. (2018) 'The Ames Stereo Pipeline: NASA's Open-Source Software for Deriving and Processing Terrain Data', *Earth and Space Science*, 5(9), pp. 537–548. Available at: <https://doi.org/10.1029/2018EA000409>
- French, Bevan.M. (1999) 'Traces of catastrophe: a handbook of shock-metamorphic effects in terrestrial meteorite impact structures', *Choice Reviews Online*, 36(10), pp. 36-5704-36-5704. Available at: <https://doi.org/10.5860/CHOICE.36-5704>
- Grin, E.A. and Cabrol, N.A. (1997) 'Subglacial Rotary Currents in Gusev Crater

Paleolake (Mars)', p. 475.

- Gwinner, K. *et al.* (2016) 'The High-Resolution Stereo Camera (HRSC) of Mars Express and its approach to science analysis and mapping for Mars and its satellites', *Planetary and Space Science*, 126, pp. 93–138. Available at: <https://doi.org/10.1016/j.pss.2016.02.014>
- Kuzmin, R.O. *et al.* (2000) *Geologic map of the MTM-15182 and MTM-15187 quadrangles, Gusev Crater-Ma'adim Vallis region, Mars*. Available at: <https://doi.org/10.3133/i2666>
- Laura, J. and Ferguson, R.L. (2016) 'Modeling martian thermal inertia in a distributed memory high performance computing environment', in *2016 IEEE International Conference on Big Data (Big Data)*. *2016 IEEE International Conference on Big Data (Big Data)*, pp. 2919–2928. Available at: <https://doi.org/10.1109/BigData.2016.7840942>
- Malin, M.C. *et al.* (2007) 'Context Camera Investigation on board the Mars Reconnaissance Orbiter', *Journal of Geophysical Research: Planets*, 112(E5). Available at: <https://doi.org/10.1029/2006JE002808>
- Milam, K.A. *et al.* (2003) 'THEMIS characterization of the MER Gusev crater landing site', *Journal of Geophysical Research: Planets*, 108(E12). Available at: <https://doi.org/10.1029/2002JE002023>
- Moratto, Z. *et al.* (2010) 'Ames Stereo Pipeline, NASA's Open Source Automated Stereogrammetry Software', *Lunar Planet. Sci. Conf.*, 41.
- Smith, D.E. *et al.* (2001) 'Mars Orbiter Laser Altimeter: Experiment summary after the first year of global mapping of Mars', *Journal of Geophysical Research: Planets*, 106(E10), pp. 23689–23722. Available at: <https://doi.org/10.1029/2000JE001364>
- Triggs, B. *et al.* (2000) 'Bundle Adjustment — A Modern Synthesis', in B. Triggs, A. Zisserman, and R. Szeliski (eds) *Vision Algorithms: Theory and Practice*. Berlin, Heidelberg: Springer Berlin Heidelberg (Lecture Notes in Computer Science), pp. 298–372. Available at: https://doi.org/10.1007/3-540-44480-7_21
- Xia, Z.H.U., Hong, L.I. and Wei, Z. (2008) 'Image Inpainting Algorithm Based on Color Region Segmentation', *Computer Engineering*, 34(14), pp. 191–193. Available at: <https://doi.org/10.3969/j.issn.1000-3428.2008.14.068>